Modelling Received Signal Strength from On-Vehicle BLE Beacons Using Skewed Distributions: A Preliminary Study

Bashar I. Ahmad†, Tohid Ardeshiri†, Pat Langdon, and Simon J. Godsill
Signal Processing and Communications Laboratory,
Engineering Department, University of Cambridge
Trumpington Street, Cambridge, UK, CB2 1PZ
Email: {bia23, ta417, pml24, sjg30}@cam.ac.uk

Thomas Popham
Research & Technology
Jaguar Land Rover
Whitley, Coventry, UK CV3 4LF
Email: tpopham@jaguarlandrover.com

***Abstract*—This paper describes a study on modelling the Received Signal Strength Indicator (RSSI) measured by the smartphone of a vehicle user. The present transmissions are emitted by dedicated radio frequency sources, such as Bluetooth Low Energy (BLE) beacons, mounted to the vehicle to determine the driver/passenger(s) proximity or relative position(s). Based on empirical data, a model of the measurements noise, which utilises skewed distributions, is proposed to capture inconsistencies in reception and the impact of occlusions on the RSSI profile in an automotive setting, for example occlusions in car parks. Experimental data is used to demonstrate the suitability of the introduced model.**

I. INTRODUCTION

Recent advances in sensing, data storage and communications technologies have led to the introduction of new smart vehicle functionalities aimed at offering a personalised and more pleasant driving experience [1]. In this context, there are substantial benefits to be gained from determining the proximity or the location of the driver relative to the vehicle, as early as possible, prior to the start of a journey. For example, activating key-fob scanner, adjusting seats as per learnt preferences, pre-configuring the infotainment system, warming/cooling the vehicle, to name a few. In this paper, we address the modelling aspect of determining the proximity or location of a vehicle user from his/her smartphone data.

There has been a growing interest in leveraging the smartphone versatile set of sensors, including a Global Navigation Satellite Systems (GNSS) receiver and Inertial Measurement Unit (IMU), for automotive applications, e.g. traffic state estimation [2], navigation [3], [4], and driver assistance [5], [6]. Whilst the ubiquitous location-based services on smartphones can enable determining the user proximity to the vehicle, their achieved location accuracy in indoor (e.g. underground or covered car parks) or even urban environments is considerably poor [7]. Aided GNSS services also have stringent power consumption and quickly drain the phone battery. This is particularly important if localisation is to be performed continuously and seamlessly without being prompted by the user. Therefore, there is a need for a cheap and power efficient solution that permits locating the smartphone of the driver/passenger relative to the vehicle.

†The first two authors made an equal contribution to this work.

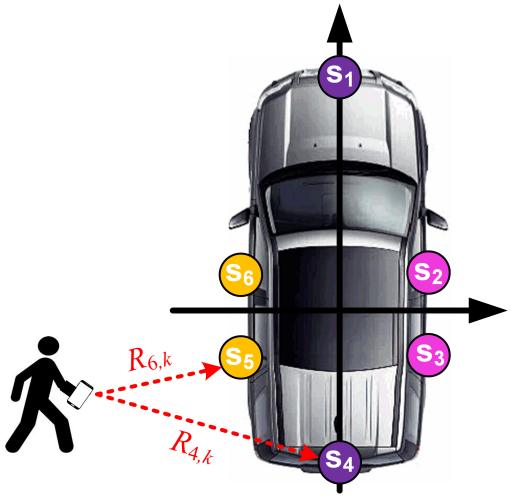

Fig. 1: Vehicle with six iBeacons, each transmitting at regular intervals.

Several alternative technologies to perform smartphone-to-vehicle positioning exist, for instance utilising the vehicle and/or smartphone IMUs [8], [9], bluetooth and audio ranging [10], wearables [11], [12], voice recognition [13], Near Field Communication (NFC) [14] and others. Majority of such solutions address locating the smartphone inside the vehicle, e.g. in the driver or passenger side. This is motivated by applications such as limiting the smartphone functionalities if it is located in the driver side to minimise distractions, identifying the driver/passenger(s), customising infotainment and others. In this study, we are primarily interested in the smartphone position (i.e. the driver/passenger location with respect to the car) whilst users approach the vehicle before starting a journey. Nevertheless, the accurate positioning of the smartphone within the vehicle can also be addressed with the same technology discussed below.

Amongst out-of-vehicle positioning solutions suitable for mobile phones and not reliant on GNSS are those based on: 1) Radio Frequency (RF) signal strength, either from RF transmissions already present (e.g. WiFi and cellular), or emitted by dedicated transmitters (e.g. installed NFC or Bluetooth transmitters), and 2) Pedestrian Dead Reckoning (PDR) from

IMU data [7]. The latter's performance can be relatively poor due to the low data quality from a typical smartphone IMU and the arbitrary position of the phone (for instance in hand, pocket, bag, etc.). This is particularly noticeable in the absence of GNSS measurements, albeit intermittent, and/or absence of detailed map information. Hence, we explore here the RF signal strength option.

In this paper, we specifically treat the problem of modelling RSSI measurements from Bluetooth low energy beacons mounted to the vehicle (e.g. see Figure 1). Data from a pilot experimental study is presented and subsequently utilised to propose as well as validate the measurements noise model. Ultimately, combining the PDR with RSSI-based methods can improve the positioning performance [7]. However, this is outside the scope of this study, whose chief purpose is to formulate a suitable RSSI measurements model that can be used in future work to enhance the driver-passenger(s) localisation from on-vehicle RF transmitters.

Employing BLE beacons or tags, namely iBeacons, is driven by their low cost, the availability of a Bluetooth receiver in most mobile phones, their remarkably low power consumption requirements and relatively long range (can be up to 200m [15]) in comparison to NFC [16]–[18]. The RSSI captures the attenuation of radio signals of known transmission powers during propagation and has been widely applied in indoor localisation systems [7], [19], [20]. Whilst RSSI can achieve relatively accurate positioning results in setups where the transmitter is in Line of Sight (LoS) and the smartphone is moving in a simple environment, it suffers from significant performance degradation in complex situations due to occlusions and multipath fading, e.g. in car parks. Thus, here we collect data from a number of on-vehicle iBeacons, namely six, to capture the effect of such occlusions. For example, Figure 1 shows vehicle with six iBeacons, one in the front and one in the back in addition to one above each of the door handles. These beacons advertise their presence, including an ID and transmitted power at 1m, every fixed interval.

The rest of the paper is organized as follows. In the next section, the common log-distance model is outlined and the modelling problem is stated. In Section III, the proposed skewed distribution measurement noise model is introduced. The experimental setup for the RSSI data collected is detailed and the proposed modelling approach is validated in Section IV. Conclusions are drawn in Section V.

II. Background and Problem Formulation

At time instant t_k, the RSSI measurement, i.e. $m_{i,k}$, pertaining to the i^{th} transmitter can be modelled by the classical log-distance model, also known as Okumura-Hata model, as per

$$z_{i,k} = P_{i,0} - \alpha_i \log(R_{i,k}) + w_k, \quad i = 1, 2, ...N, \qquad (1)$$

where $P_{i,0}$ is the transmitted power in dB (including at a fixed distance, e.g. 1m, thus, incorporating antenna gain, etc.), α_i is the path loss coefficient and $R_{i,k} = \|p(t_k) - s_i\|_2$ is the range such that $p(t_k)$ and s_i are the locations of the smartphone and the i^{th} transmitter, respectively [7], [21]; 2-dimensional coordinates of positions are assumed throughout this paper. Whereas, w_k represents the noise due to the shadowing effects and possibly occlusions. The simple model in (1) is one of the most commonly used path loss models and it is adopted here.

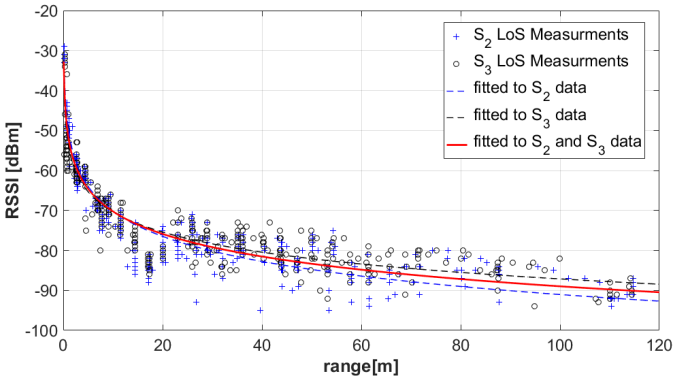

(a) Line of sight measurements.

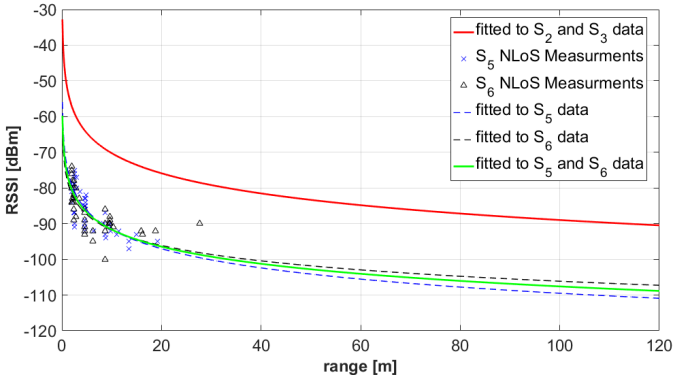

(b) Non-line of sight measurements.

Fig. 2: Fitted log-distance model for various ranges.

A Gaussian measurement noise, $w_k \backsim \mathcal{N}(0, \Sigma)$, in (1) is often assumed, i.e. it has a symmetric distribution [7], [19]. The objective of this study is to show from experimental data that due to occlusions and the Non-Line of Sight (NLoS) measurements from one or more of the N transmitters, the Gaussian assumption does not hold in the addressed automotive application. Instead, a skewed distribution model is proposed. Capturing the impact of NLoS measurements using a skewed distribution has the potential to lead to significantly more accurate location/proximity estimates, for instance see [22] where a *skew-t* likelihood is incorporated for time-of-arrival measurements.

Figure 2 shows the model in (1) fitted, via linear regression, to a limited set of RSSI data measured by a smartphone from four beacons (two on each side of the vehicle, see Figure 1); the smartphone position (i.e. range) is accurately known. Further details on the setup are given in Section IV. The phone logs simultaneously the LoS (e.g. from beacons S_2 and S_3 on the driver side in Figure 1) and NLoS (e.g. from beacons S_5 and S_6 on the front passenger side, which is the right hand side in the UK) at several ranges; no obstacles exist between

the smartphone and vehicle. It can be easily seen from Figure 2a that the model in (1) is representative of the recorded LoS data with observations up to 120m away. Whereas, for the beacons occluded by the vehicle most of the measurements are collected within a 20m range and the previously fitted model is not applicable.

III. Proposed Modelling Framework for noise

Since the maximum received power cannot exceed that transmitted by the BLE beacon, it is intuitive to assume that the RSSI noise can only belong to a limited range of positive values. Whereas, due to occlusions, RF signal can be substantially attenuated and, thereby, the likelihood of w_t in (1) taking large negative values should be captured by the model. This implies that a skewed distribution, rather than a symmetric one, which is more heavy tailed to the left hand side, is expected to better model the measurement noise in the addressed automotive application. In this paper, we proposed modelling the RSSI measurements from different beacons as independently univariate skewed distributions. A distribution that is particularly suitable is univariate skew-t, which is described below for completeness, see [22]–[24] for more details.

The univariate skew t-distribution is parameterised by its location parameter $\mu \in \mathbb{R}$, spread parameter $\sigma \in \mathbb{R}^+$, shape parameter $\delta \in \mathbb{R}$ and degrees of freedom $\nu \in \mathbb{R}^+$. Its Probability Density Function (PDF) is described by

$$\mathrm{ST}(z; \mu, \sigma^2, \delta, \nu) = 2\,\mathrm{t}(z; \mu, \delta^2 + \sigma^2, \nu)\,\mathrm{T}(\widetilde{z}; 0, 1, \nu + 1), \tag{2}$$

such that $\mathrm{t}(z; \mu, \sigma^2, \nu)$is the PDF of Student's t-distribution, and $\widetilde{z}$ is defined by

$$\widetilde{z} \triangleq \frac{(z-\mu)\delta}{\sigma}\sqrt{\frac{\nu+1}{\nu(\delta^2+\sigma^2)+(z-\mu)^2}}. \tag{3}$$

Whereas, the Cumulative Distribution Function (CDF) of Student's t-distribution with degrees of freedom ν and scale 1 is denoted by $\mathrm{T}(\widetilde{z}; 0, 1, \nu)$. The skew t-distribution, according to the definitions in (2)-(3), was originally introduced in the multivariate form in [25]–[27]. Furthermore, expressions for the first two moments of the univariate skew t-distribution with the parameterisation in (2) can be found in [28], [29].

In Figure 3 the PDF of $\mathrm{ST}(z; 0, 1, \delta, 4)$ is plotted for three values of δ, and in Figure 4 the PDF of $\mathrm{ST}(z; 0, 1, 1, \nu)$ is displayed for three values of ν. It can be noticed that increasing δ increases its skewness, whereas decreasing ν increases the distribution heavy-tailedness.

A useful representation of the skew t-distribution is the hierarchical representation [30]

$$z|u, \lambda \sim \mathcal{N}(\mu + \delta u, \lambda^{-1}\sigma^2), \tag{4a}$$

$$u|\lambda \sim \mathcal{N}_+(0, \lambda^{-1}), \tag{4b}$$

$$\lambda \sim \mathcal{G}\left(\frac{\nu}{2}, \frac{\nu}{2}\right), \tag{4c}$$

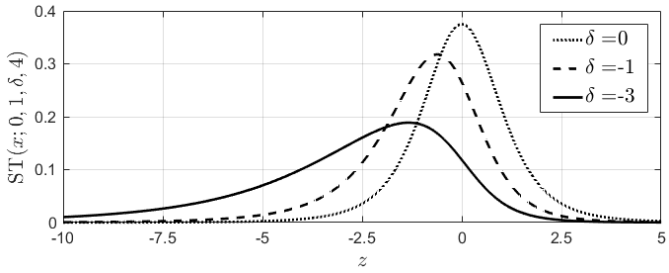

Fig. 3: The PDF of $\mathrm{ST}(x; 0, 1, \delta, 4)$ for different values of δ; $\delta = 0$ gives Student's t-distribution, and increasing δ increases the skewness.

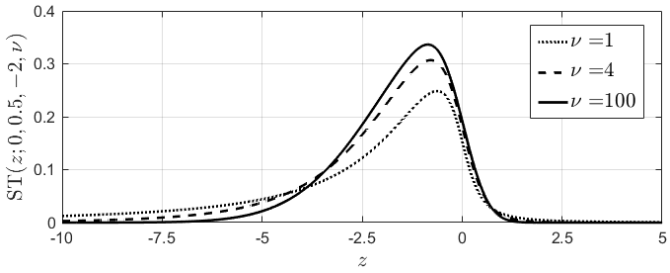

Fig. 4: The PDF of $\mathrm{ST}(z; 0, 0.5, -2, \nu)$ for different values of ν; $\nu = \infty$ gives the skew normal distribution, and decreasing ν increases heavy-tailedness.

where u and λ are scalar random variables and $\mathcal{N}_+(m, s^2)$ denotes the truncated normal distribution with closed positive orthant as support, location parameter m, and scale-parameter s. Furthermore, $\mathcal{G}(\alpha, \beta)$ is the gamma distribution with shape parameter α and rate parameter β. The hierarchical representation (4) can be used to generate samples from the skew t-distribution for parameter inference for fitting likelihood functions as well as approximate filtering and smoothing using variational Bayes as in [22] and [23]. The parameters of the skew t-distribution can also found using the maximum likelihood principle. That is for J independent measurements with known true values and error z^j the parameter $\Omega \triangleq \left\{\mu, \sigma^2, \delta, \nu\right\}$ is given by

$$\hat{\Omega} = \arg\max_{\Omega} \prod_{j=1}^{J} \mathrm{ST}(z^j \mid \Omega) \tag{5}$$

which can be solved by a gradient based optimization solver and others, e.g. [31].

Although skewed t-distribution was described in this section, other skewed distribution such as skew normal, Rayleigh, gamma and mixture distribution, e.g. Gaussian mixtures, can be utilised; several distributions are examined in Section IV-B. Whilst the resultant likelihoods for all these distributions can be used in a particle filter or analytical sequential filters within a Bayesian filtering framework, [23], [24] offer a filtering and a smoothing framework using variational Bayes method for skew t likelihood. Whereas, skew normal likelihood requires a moment matching step in its measurement update. Gaussian

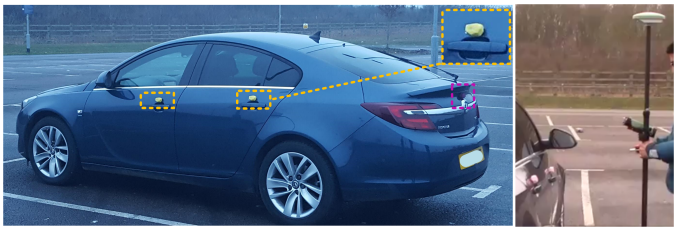

Fig. 5: The vehicle used in the experiment. The three visible beacons (out of the six) are indicated by the colored squares in the left picture. The right picture depicts the portable RTK satellite navigation system (Leica GS08+) held by the user.

mixture filtering methods entail a mixture reduction step [32]. We recall that the inference aspect is outside the scope of this paper.

IV. Experimental Validation

A. Set-up and Data Collection Procedure

In this study, data is collected simultaneously from six iBeacons [16] mounted around a Vauxhall Insignia car as per Figure 1 using a Samsung Galaxy S6 smartphone. Estimote Long Range Beacons are employed here [15]; they have a long coverage with reconfigurable advertisement interval T and transmitted power (set at 10dBm). Additionally, a Leica GS08+ RTK satellite navigation system is utilised to obtain accurate position/range measurements of the smartphone/vehicle-user, hence produces ground-truth positioning data. It has a reliable horizontal and vertical accuracies (pole height is 1.5m) of 5mm and 10mm , respectively. Figure 5 depicts the vehicle with the beacons as well as the portable RTK satellite navigation system held by the user.

Whilst at least two (out of the six) beacons are occluded at any point in time (i.e. without a LoS with the smartphone) by the test vehicle, the RSSI and RTK data is collected in a large empty car park. Nevertheless, the scenario where a car is parked next to the test vehicle with beacons is also considered as shown in Figure 6. The smartphone collects data from all six beacons every, approximately, 1.2 seconds (i.e. six RSSI observations from all six beacons), whereas the RTK system data rate is approximately 1Hz. Figure 7 depicts the layout of the overall track sampled by the smartphone. It pertains to experiments collected over three full days, where the user is constantly moving in the vicinity of the vehicle for considerable durations. After sorting and removing ambiguities (e.g. due to intermittent loss of the RTK service and smartphone system interruptions), over 140min of continuous measurements are extracted. All positioning data is rotated, converted to meters and aligned with the test vehicle, which represents the origin as can be noticed from Figures 7.

It is worth noting that it is inevitable that the user's body as well as hand holding the smartphone, and the RTK system pole might, sometimes (however infrequent), obstruct the smarphone's direct line of sight to the beacons, especially given the length of the conducted experiments. Therefore, LoS

Fig. 6: Occluded scenario with a car parked on the right hand side of the vehicle instrumented with iBeacons.

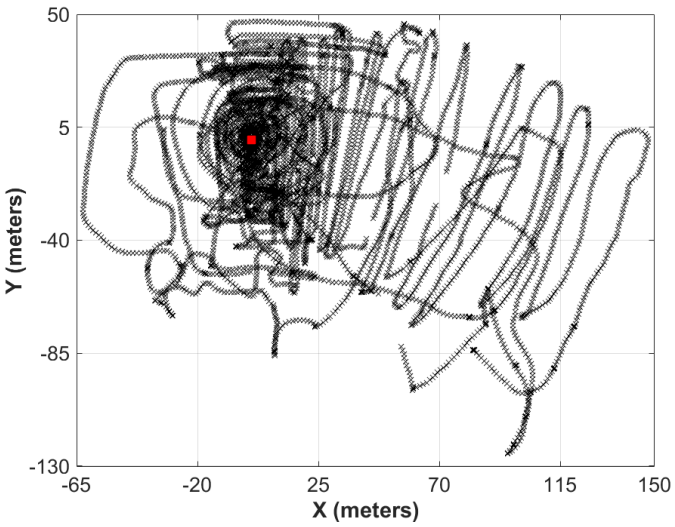

Fig. 7: The layout of the overall track sampled by the smartphone (red square is the test vehicle with beacons).

describe the scenario where no major physical object (e.g. vehicle) is obstructing the smartphone-beacon line of sight.

B. Data Analysis

Figure 8 exhibits the coverage area of each of the six sensors/beacons in the empty car park scenario. Due to physical restrictions of the car park (e.g. size-shape), the areas to the right and rear of the car are sampled more densely and at longer ranges as seen in the figure. Nonetheless, assuming symmetry between the left and right sides of the car as well as between front and the rear, the measurements can be mirrored to create a symmetrical surveyed area around the car. The following observations are made from Figure 8: 1) the sensor range can be up to 140m in LoS (see sub-plot for beacon S_4) and up to 20m in NLoS conditions, 2) the measurements are significantly more dense near the car and they become gradually sparse as the range smartphone departs from the car, and 3) front and back beacons have the widest coverage areas. It is also expected that a car parked to the right or left of the test vehicle will have a similar impact to that seen in the NLoS region per beacon in Figure 8 (i.e. reduce coverage region).

Since the accurate position of the smartphone is available via the RTK system (albeit the system's remarkably low

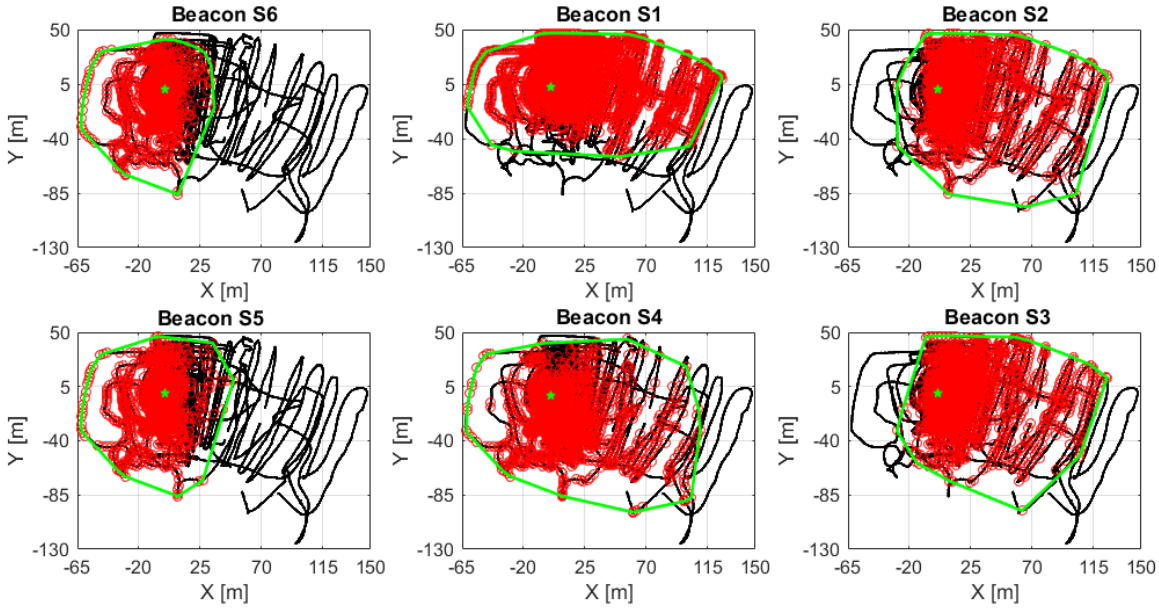

Fig. 8: Sensor coverage area for each beacon (S_1 to S_6, each in a sub-plot). The black line-with-dots is the smartphone location as per the GPS, red circles are the location of the RSSI measured by a smartphone for each beacon, green star is the beacon location and green polygon represents the convex hull of the position of RSSI measurements from each beacon.

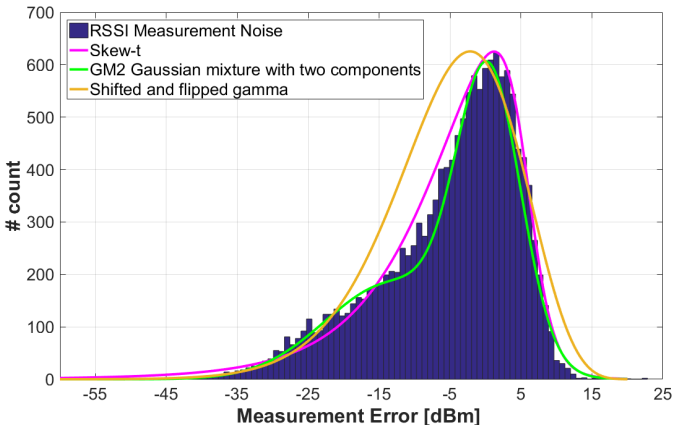

Fig. 9: Histogram of the RSSI measurements noise from all six beacons and logged data points; various skewed distributions fitted to data are shown.

localisation uncertainty), the RSSI measurements error w_t can be calculated directly from (1). Figure 9 depicts the histogram of the measurements noise/error from all of the collected RSSI data. The figure also shows a few suitable asymmetric/skewed distributions that can be fitted, e.g. see the ML criterion in (5), to the empirical log RSSI measurements noise. Namely, the figure displays the fitted distributions (from): a) skew-t, b) gamma (shifted and flipped to represent the negative values as well as the skewness to the left hand side), and c) Gaussian mixture model with two components; Rayleigh is not shown here due to the poor fit. Whereas, Figure 10 exhibits the histogram of the noise for the LoS and NLoS measurements separately.

It can be noticed from Figure 9 that the measurements noise distribution is clearly asymmetric with notable skewness to the left due to the impact of occlusions and possibly fading. Thus, it cannot be easily modelled by a Gaussian distribution. The skew t-distribution discussed in Section III closely fits the data in Figure 9. It is a strong candidate for devising a suitable inference routine to establish the range or relative position of the smartphone using data from all the available sensors/beacons, e.g. see [22], [23]. Furthermore, the proposed skewed likelihood functions can be used in a Sequential Monte Carlo framework also known as particle filtering. This aspect will be addressed in future work. As expected, Figure 10 also shows that more samples are visible in LoS, albeit including possible obstructions by the user's hand, etc. Whereas, the NLoS error is nearly symmetric, see the coverage areas analysis in Figure 8. Combining the LoS and NLoS results in the skewness of the noise distribution.

Finally, to demonstrate the difficulties that can arise from directly inferring the range from the RSSI measurements model in (1), i.e.

$$\hat{R}_{i,k} = \exp\left(\frac{z_{i,k} - P_{i,0}}{-\alpha_i}\right), \tag{6}$$

and without *a priori* knowledge of the LoS and NLoS measurements as is the case in practice, Figure 11 shows the Okumura-Hata model fitted to the overall logged data. It is clear from Figure 11 that the measurements model can notably misrepresent the position/range information due to noise and occlusions. Error in the range estimates from (6) can be in the

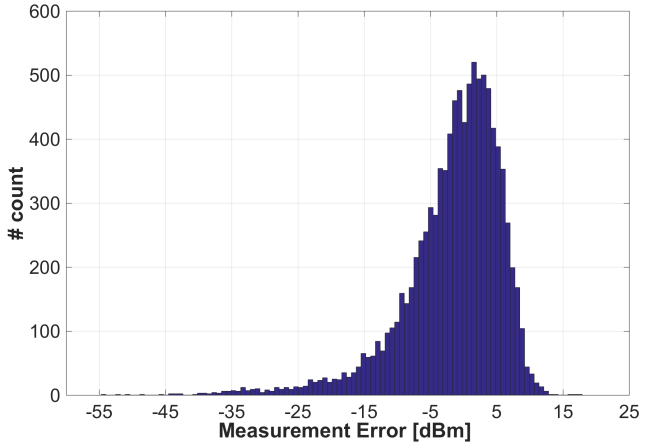

(a) Line of sight.

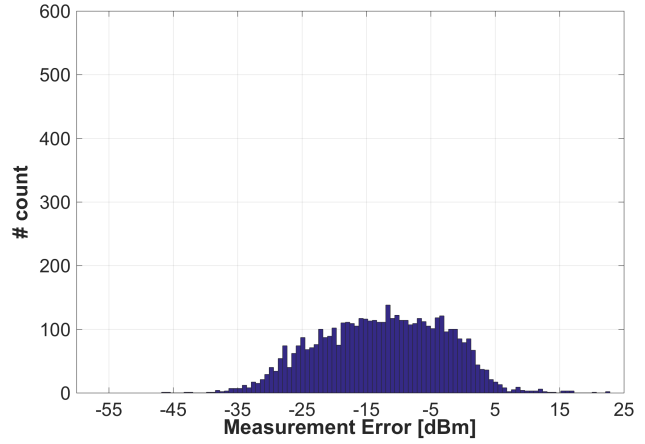

(b) Non-line of sight.

Fig. 10: RSSI measurement noise from LoS and NLoS beacons (together they form the data in Figure 9).

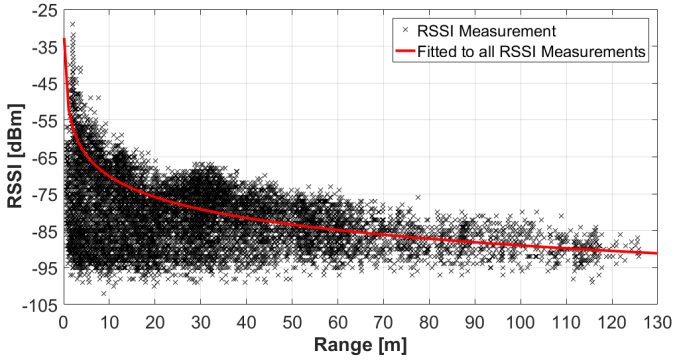

Fig. 11: Log-distance model from all collected data from six beacons (i.e. LoS and NLoS data).

region of 50m up to 100m from the data in Figure 11.

C. Final Remarks

Occlusions can also be induced by any other objects or material obstructing the smartphone-beacon LoS, for instance, car park pillars, other pedestrians, and/or if the phone is in the user's pocket, handbag, etc. Moreover, the locations of the RF sources on the vehicle can be modified, e.g. a beacon mounted to the car roof can have a wider coverage area; the use of six beacons was in fact motivated by covering the majority of the driver/passenger(s) approach directions. It is noted that to be able to locate the user with respect to the vehicle (i.e. not only estimating range), data from the available beacons (preferably all) need to be fused and several well-established fusion techniques from wireless sensor network and tracking areas exist. Nevertheless, most approaches assume a symmetric measurement noise models or even adopt a deterministic formulation, e.g. see [33] for an overview.

Whilst in this paper a pilot experimental study is conducted focusing on data modelling, it presents a clear indication that skewed distributions present themselves as strong candidates to accurately model the RSSI measurement noise from BLE transmitters (or any other RF source) in automotive settings. Thereby, such models can potentially achieve more accurate localisation results. In this context, occlusions can even be employed as a feature to enhance localisation from a number of beacons with varying coverage areas, rather than being treated as a nuisance.

V. Conclusions

Data from an experimental study with on-vehicle BLE beacons is presented and a skewed distribution model of the RSSI measurement noise is proposed. This skewness is demonstrated utilising the collected empirical data. This preliminary study serves the purpose of motivating and paving the way for formulating an inference framework that incorporates or even exploits this skewness in the RSSI profile induced by occlusions and multipath fading in automotive applications. Such an inference framework is expected to outperform algorithms which assume a symmetrical noise distribution such as nonlinear least squares type and Kalman filter type algorithms.

Subsequent work can leverage this information (e.g. assume a skew t-distributed measurement noise in lieu of the common Gaussian model) to achieve more accurate estimations of the driver/passengers location with respect to vehicle using RSSI measurements from on-vehicle beacons and possibly utilising built-in smartphone sensors, such as the inertia measurement unit.

Acknowledgment

The authors would like to thank Jaguar Land Rover, for funding this work under the Centre for Advanced Photonics and Electronics (CAPE) agreement.

References

[1] R. Bishop, *Intelligent vehicle technology and trends*, 2005.

[2] R. Ansar, P. Sarampakhul, S. Ghosh, N. Mitrovic, M. T. Asif, J. Dauwels, and P. Jaillet, "Evaluation of smart-phone performance for real-time traffic prediction," in *Intelligent Transportation Systems (ITSC), 2014 IEEE 17th International Conference on*. IEEE, 2014, pp. 3010–3015.

[3] P. Hao, K. Boriboonsomsin, G. Wu, and M. Barth, "Probabilistic model for estimating vehicle trajectories using sparse mobile sensor data," in *2014 IEEE 17th International Conference on Intelligent Transportation Systems (ITSC)*. IEEE, 2014, pp. 1363–1368.

[4] X. Niu, Q. Zhang, Y. Li, Y. Cheng, and C. Shi, "Using inertial sensors of iphone 4 for car navigation," in *Position Location and Navigation Symposium (PLANS), 2012 IEEE/ION*. IEEE, 2012, pp. 555–561.

[5] D.-W. Koh and H.-B. Kang, "Smartphone-based modeling and detection of aggressiveness reactions in senior drivers," in *Intelligent Vehicles Symposium (IV), 2015 IEEE*. IEEE, 2015, pp. 12–17.

[6] K. Bengler, K. Dietmayer, B. Farber, M. Maurer, C. Stiller, and H. Winner, "Three decades of driver assistance systems: Review and future perspectives," *IEEE Intelligent Transportation Systems Magazine*, vol. 6, no. 4, pp. 6–22, 2014.

[7] P. Davidson and R. Piche, "A survey of selected indoor positioning methods for smartphones," *IEEE Communications Surveys & Tutorials*, 2016.

[8] J. Wahlström, I. Skog, P. Händel, and A. Nehorai, "Imu-based smartphone-to-vehicle positioning," *IEEE Transactions on Intelligent Vehicles*, vol. 1, no. 2, pp. 139–147, 2016.

[9] Z. He, J. Cao, X. Liu, and S. Tang, "Who sits where? infrastructure-free in-vehicle cooperative positioning via smartphones," *Sensors*, vol. 14, no. 7, pp. 11 605–11 628, 2014.

[10] J. Yang, S. Sidhom, G. Chandrasekaran, T. Vu, H. Liu, N. Cecan, Y. Chen, M. Gruteser, and R. P. Martin, "Sensing driver phone use with acoustic ranging through car speakers," *IEEE Transactions on Mobile Computing*, vol. 11, no. 9, pp. 1426–1440, 2012.

[11] A. Mariakakis, V. Srinivasan, K. Rachuri, and A. Mukherji, "Watchudrive: Differentiating drivers and passengers using smartwatches," in *2016 IEEE International Conference on Pervasive Computing and Communication Workshops*. IEEE, 2016, pp. 1–4.

[12] L. Liu, C. Karatas, H. Li, S. Tan, M. Gruteser, J. Yang, Y. Chen, and R. P. Martin, "Toward detection of unsafe driving with wearables," in *Proceedings of the 2015 workshop on Wearable Systems and Applications*. ACM, 2015, pp. 27–32.

[13] M. Feld, T. Schwartz, and C. Müller, "This is me: using ambient voice patterns for in-car positioning," in *International Joint Conference on Ambient Intelligence*. Springer, 2010, pp. 290–294.

[14] H. Chu, V. Raman, J. Shen, A. Kansal, V. Bahl, and R. R. Choudhury, "I am a smartphone and i know my user is driving," in *Communication Systems and Networks (COMSNETS), 2014 Sixth International Conference on*. IEEE, 2014, pp. 1–8.

[15] Estimote, *Accessed on 29/01/2017: http://estimote.com/.*

[16] iBeacon for developers, *Accessed on 29/01/2017: https://developer.apple.com/ibeacon/.*

[17] P. Martin, B.-J. Ho, N. Grupen, S. Muñoz, and M. Srivastava, "An ibeacon primer for indoor localization: demo abstract," in *Proceedings of the 1st ACM Conference on Embedded Systems for Energy-Efficient Buildings*. ACM, 2014, pp. 190–191.

[18] Z. Jianyong, L. Haiyong, C. Zili, and L. Zhaohui, "Rssi based bluetooth low energy indoor positioning," in *2014 International Conference on Indoor Positioning and Indoor Navigation (IPIN)*. IEEE, 2014, pp. 526–533.

[19] H. Nurminen, J. Talvitie, S. Ali-Loytty, P. Muller, E. Lohan, R. Piché, and M. Renfors, "Statistical path loss parameter estimation and positioning using rss measurements," in *Ubiquitous Positioning, Indoor Navigation, and Location Based Service (UPINLBS), 2012*. IEEE, 2012, pp. 1–8.

[20] J. J. Diaz, R. d. A. Maues, R. B. Soares, E. F. Nakamura, and C. M. Figueiredo, "Bluepass: An indoor bluetooth-based localization system for mobile applications," in *Computers and Communications (ISCC), 2010 IEEE Symposium on*. IEEE, 2010, pp. 778–783.

[21] M. Hata, "Empirical formula for propagation loss in land mobile radio services," *IEEE transactions on Vehicular Technology*, vol. 29, no. 3, pp. 317–325, 1980.

[22] H. Nurminen, T. Ardeshiri, R. Piché, and F. Gustafsson, "A nlos-robust toa positioning filter based on a skew-t measurement noise model," in *International Conference on Indoor Positioning and Indoor Navigation (IPIN)*. IEEE, 2015, pp. 1–7.

[23] H. Nurminen, T. Ardeshiri, R. Piché, and F. Gustafsson, "Robust inference for state-space models with skewed measurement noise," *IEEE Signal Processing Letters*, vol. 22, no. 11, pp. 1898–1902, November 2015.

[24] H. Nurminen, T. Ardeshiri, R. Piché, and F. Gustafsson, "Skew-t filter and smoother with improved covariance matrix approximation," *CoRR*, vol. abs/1608.07435, 2016. [Online]. Available: http://arxiv.org/abs/1608.07435

[25] M. D. Branco and D. K. Dey, "A general class of multivariate skew-elliptical distributions," *Journal of Multivariate Analysis*, vol. 79, no. 1, pp. 99–113, October 2001.

[26] A. Azzalini and A. Capitanio, "Distributions generated by perturbation of symmetry with emphasis on a multivariate skew t-distribution," *Journal of the Royal Statistical Society. Series B (Statistical Methodology)*, vol. 65, no. 2, pp. 367–389, 2003.

[27] A. K. Gupta, "Multivariate skew t-distribution," *Statistics*, vol. 37, no. 4, pp. 359–363, 2003.

[28] S. K. Sahu, D. K. Dey, and M. D. Branco, "A new class of multivariate skew distributions with applications to Bayesian regression models," *Canadian Journal of Statistics*, vol. 31, no. 2, pp. 129–150, 2003.

[29] ——, "Erratum: A new class of multivariate skew distributions with applications to Bayesian regression models," *Canadian Journal of Statistics*, vol. 37, no. 2, pp. 301–302, 2009.

[30] T.-I. Lin, "Robust mixture modeling using multivariate skew t distributions," *Statistics and Computing*, vol. 20, pp. 343–356, 2010.

[31] S. X. Lee and G. J. McLachlan, "EMMIXuskew: An R package for fitting mixtures of multivariate skew t distributions via the EM algorithm," *Journal of Statistical Software*, vol. 55, no. 12, pp. 1–22, 11 2013.

[32] T. Ardeshiri, K. Granström, E. Özkan, and U. Orguner, "Greedy reduction algorithms for mixtures of exponential family," *IEEE Signal Processing Letters*, vol. 22, no. 6, pp. 676–680, 2015.

[33] F. Gustafsson, *Statistical sensor fusion*. Studentlitteratur, 2010.